Three-dimensional Z-pinch wire array modeling

Allen C. Robinson

Computational Physics R&D (9231)

Christopher J. Garasi

HEDP Theory/ICF Target Design (1674)

Sandia National Laboratories

Poster presented at 18th International Conference on Numerical Simulation of Plasmas

Cape Cod, Massachusetts, USA

Sept 7-10, 2003

Sandia is a multiprogram laboratory operated by Sandia Corporation, a Lockheed Martin Company, for the United States Department of Energy's National Nuclear Security Administration under contract DE-AC04-94AL85000.

Sandia National Laboratories

Simulations in Support of Sandia's Z-facility

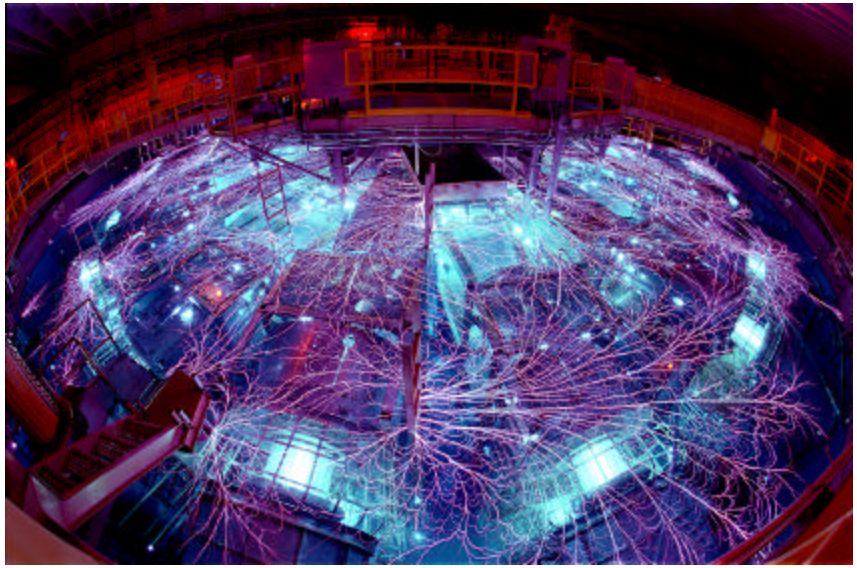

Marx generators
11.4 MJ/1 µs

Hundreds of micron-radius wires

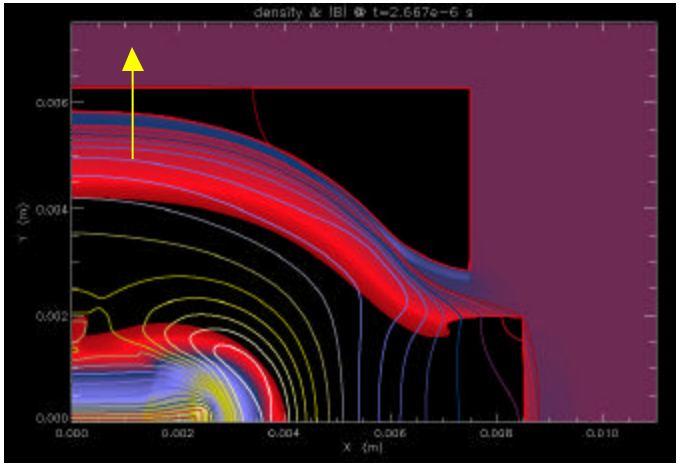

Magnetically propelled flyer plates

ALEGRA-HEDP

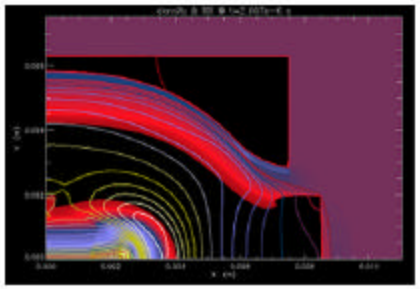

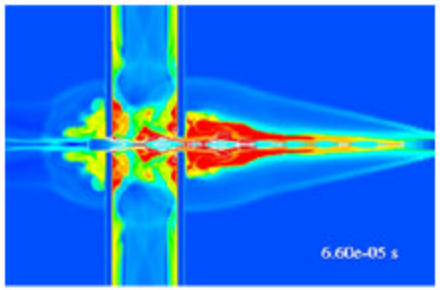

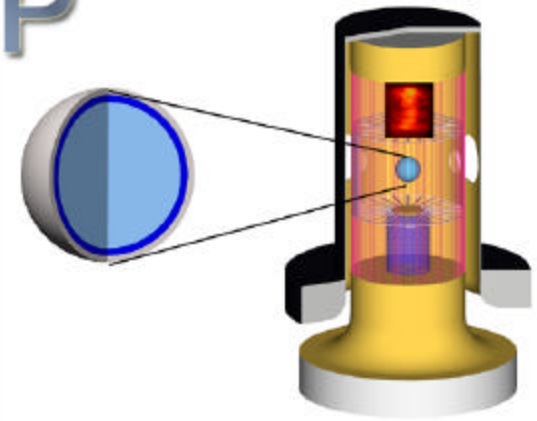

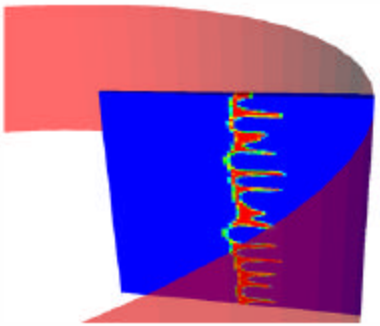

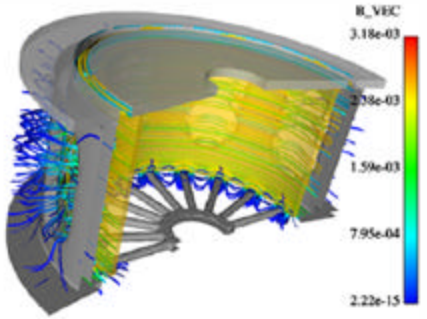

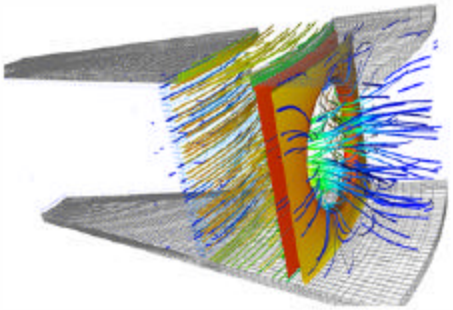

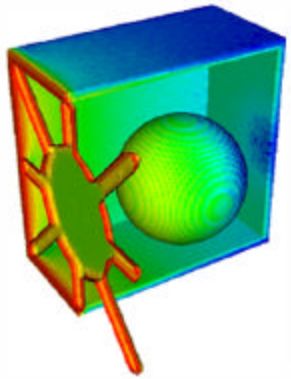

Features

2D (RZ & XY) & 3D (XYZ)
Unstructured Finite Element
Object Oriented
Parallelized (massively parallel)
Multi-material ALE
Coupled Physics
- hydrodynamics
- resistive MHD
- radiation transport
- thermal conduction

High Energy Density Physics

Arbitrary Lagrangian-Eulerian (ALE) sequence for ALEGRA-MHD

- **2D and 3D multiple material ALE based on unstructured mesh hex and quad finite elements.**
- **Lagrangian Steps (Operator split)**
  - **Compute forces and accelerations**
  - **Move nodes (magnetic fluxes or magnetic potential circulations are invariant)**
  - **Implicit magnetic diffusion (eddy currents) and Joule heating, energy transfer through boundary. Vacuum is approximated with a very small conductivity.**
- **Remesh - Chose a close new mesh**
- **Remap Step**
  - **compute new values at element centers, nodes, faces and edges. Constrained transport for face centered fluxes.**

Invariants of motion in ideal Lagrangian MHD

- **Conservation of Magnetic Flux**

$$\oint_{\partial V} \mathbf{B} \bullet d\mathbf{a} = 0$$

- **Faraday's Law**

$$\mathbf{B} = \nabla \times \mathbf{A}$$

$$\frac{d}{dt} \int_{S(t)} \mathbf{B} \bullet d\mathbf{a} + \oint_{\partial S} \mathbf{E} \bullet d\mathbf{x} = 0 \qquad \frac{d}{dt} \oint_{\partial S(t)} A \bullet d\mathbf{x} + \oint_{\partial S} \mathbf{E} \bullet d\mathbf{x} = 0$$

- **Magnetic flux and vector potential circulation are invariants in ideal MHD. This leads to a natural operator split for Faraday's law. Move the nodes assuming a constant flux, then solve a standard diffusion equation at the new location. The term in red below is zero by algorithmic construction.**

$$\int_{S(t+\Delta t)} \frac{\mathbf{B}(\mathbf{x}, t+\Delta t) - \mathbf{B}(\mathbf{x}, t)}{\Delta t} \bullet d\mathbf{a}^{n+1} + \oint_{\partial S(t+\Delta t)} \mathbf{E} \bullet d\mathbf{x}^{n+1}$$

$$+ \frac{1}{\Delta t} \left(\int_{S(t+\Delta t)} \mathbf{B}(\mathbf{x}, t) \bullet d\mathbf{a}^{n+1} - \int_{S(t)} \mathbf{B}(\mathbf{x}, t) \bullet d\mathbf{a}^{n} \right) = 0$$

Transient magnetics (eddy current) equations solved using edge/face FE

Ω = a single conducting region in $\hat{A}^3$.

weakly enforced

$$\nabla \times \mathbf{H} = \mathbf{J} \qquad \frac{\partial \mathbf{B}}{\partial t} + \nabla \times \mathbf{E} = 0 \quad \text{Exact relationship}$$

$$\nabla \bullet \mathbf{J} = 0 \qquad \nabla \bullet \mathbf{B} = 0$$

$$\mathbf{B} = m\,\mathbf{H} \qquad \mathbf{J} = s\,\mathbf{E}$$

boundary conditions $\begin{cases} \mathbf{E} \times \mathbf{n} = \mathbf{E}_b \times \mathbf{n} \text{ on } \Gamma_1 (\textit{Dirichlet}), \\ \mathbf{H} \times \mathbf{n} = \mathbf{H}_b \times \mathbf{n} \text{ on } \Gamma_2 (\textit{Neumann}) \end{cases}.$

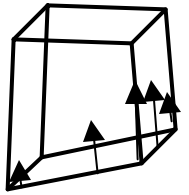

Edge element

$$\int s\,\mathbf{E}^{n+1} \bullet \hat{\mathbf{E}} dV + \Delta t \int \frac{\text{curl}\,\mathbf{E}^{n+1} \bullet \text{curl}\,\hat{\mathbf{E}}}{m} dV = \int \frac{\mathbf{B}^n \bullet \mathbf{curl}\hat{\mathbf{E}}}{m} dV - \int \mathbf{H}_b \times \mathbf{n} \bullet \hat{\mathbf{E}} dA$$

B = magnetic flux density **E** = electric field **H** = magnetic field

m = permeability s = conductivity **J** = current density

m and s positive and finite everywhere in Ω

Magnetics Numerical Algorithm

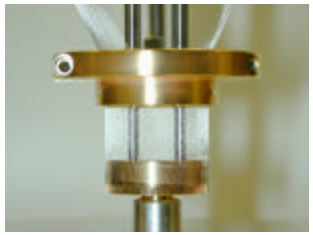

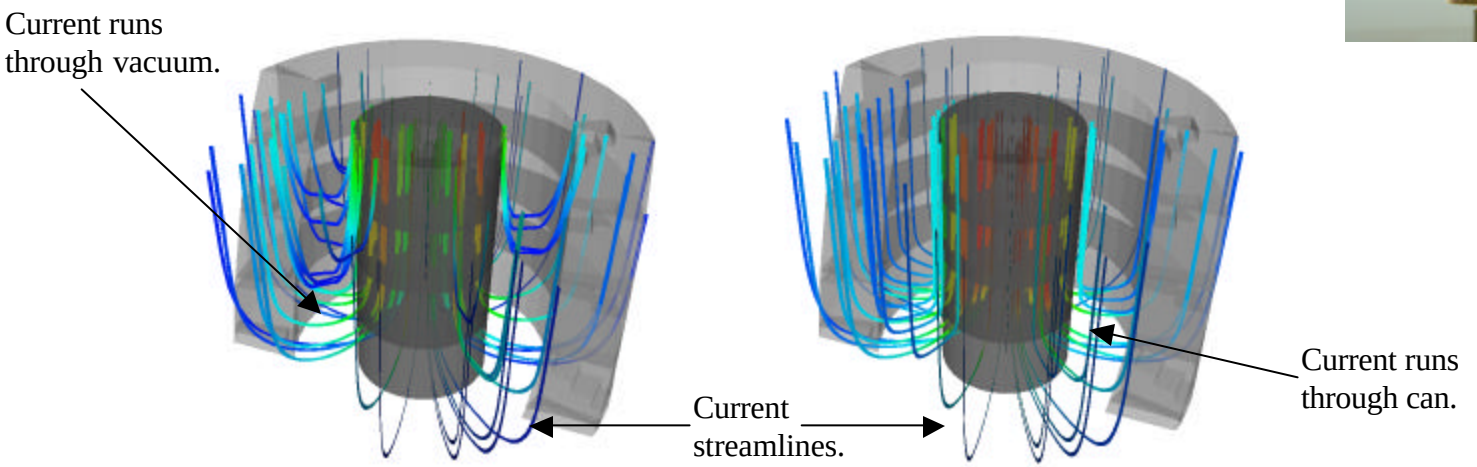

Nodal Formulation Result
(poor current distribution)

Edge Formulation Result
(accurate current distribution)

- Extreme variations (~10^6-10^8) in material properties & spatial scale pose considerable difficulty for magnetic field solution
- Edge-based discretization required.
- Multilevel matrix solver designed specifically for curl curl operator

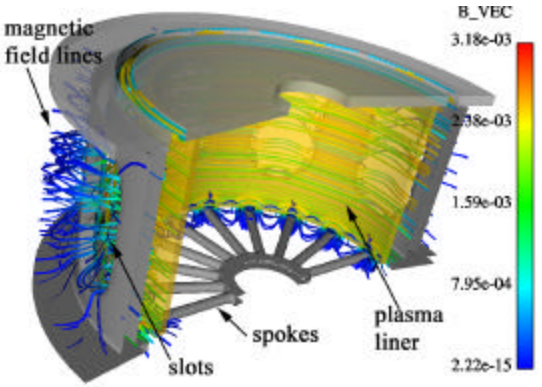

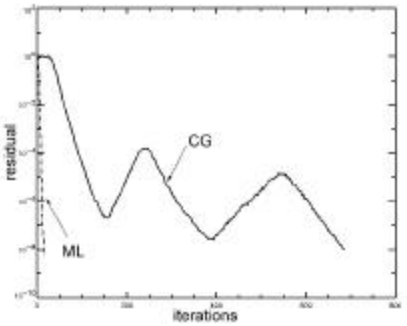

H(curl) AMG

- Algebraic multigrid (AMG) iteratively solves $Ax = b$ scalably by accelerating solve with "coarse grid" matrices
  - Interpolation & restriction operators move information between grids
    - » $\mathbf{R_k} = \mathbf{I_k}^T$
    - » $\mathbf{A_{k-1}} = \mathbf{R_{k-1}}\,\mathbf{A_k}\,\mathbf{I_{k-1}}$ (Galerkin coarsening)

Comple-mentary

  - Smoother: simple solver reduces high energy error on each level
  - Coarse grid correction: reduces low energy error
- H(curl): discrete gradients are null space of discrete curl

  ⇒ (near) null space dimension is large (≈ grid nodes)

- Smoother: distributed relaxation (Hiptmair, Brandt)
  - 1) Sweep over $Ax=b$, 2) project residual into near null space & sweep over projected system, 3) project back & update solution
  - Chebyshev polynomial smoothing is used in both sweeps and gives parallel independence since kernels are matrix-vector operations.

Coarse Grid Correction

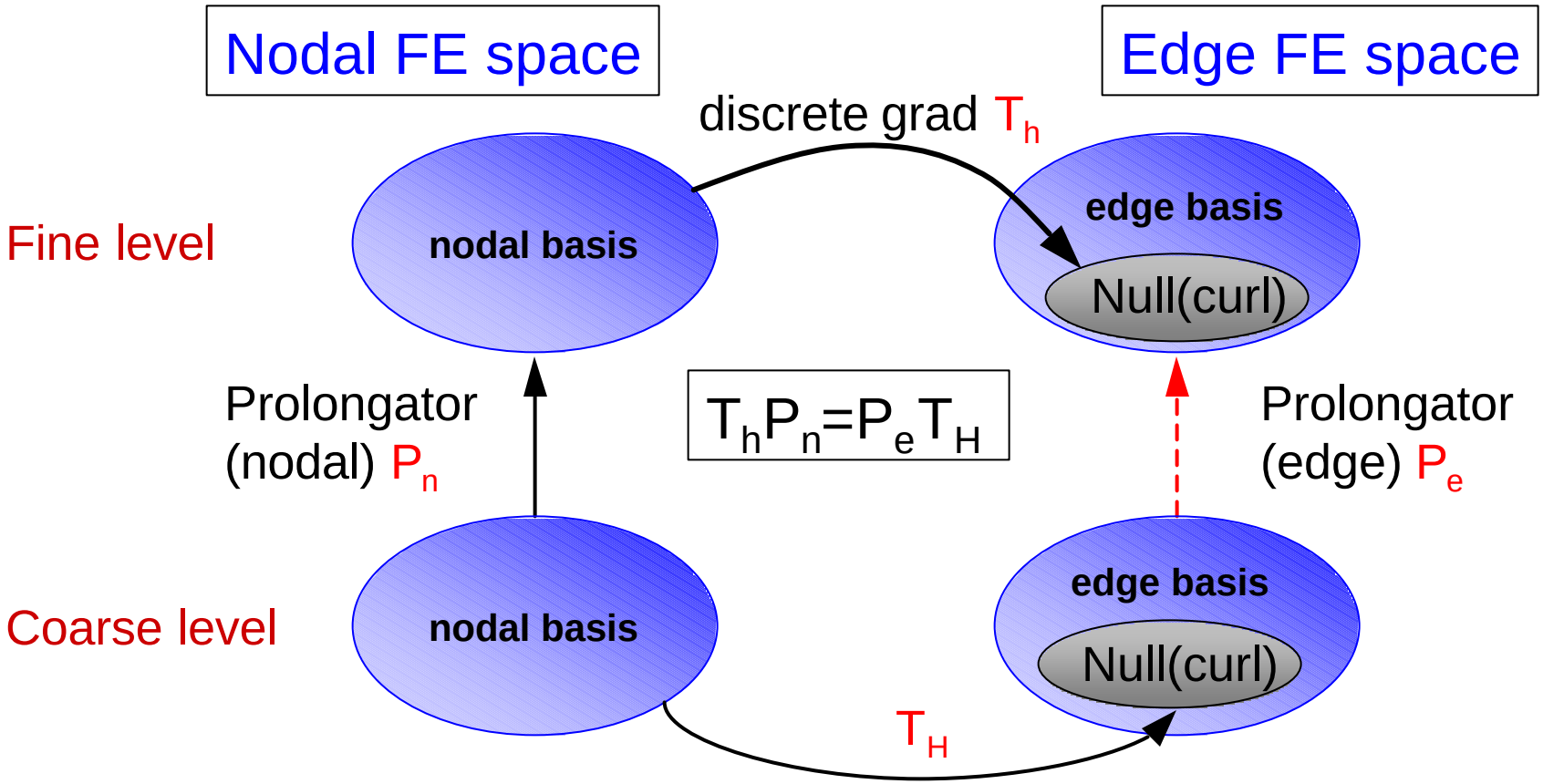

If $S_hT_h = 0$ and $S_H = P_e{}^TS_hP_e$, then $T_hP_n=P_eT_H \Rightarrow S_HT_H = 0$, i.e., curl/grad relationship holds on coarser level H.

h-independence in Model Problems

2D Box, $\sigma = 10^{-3}$

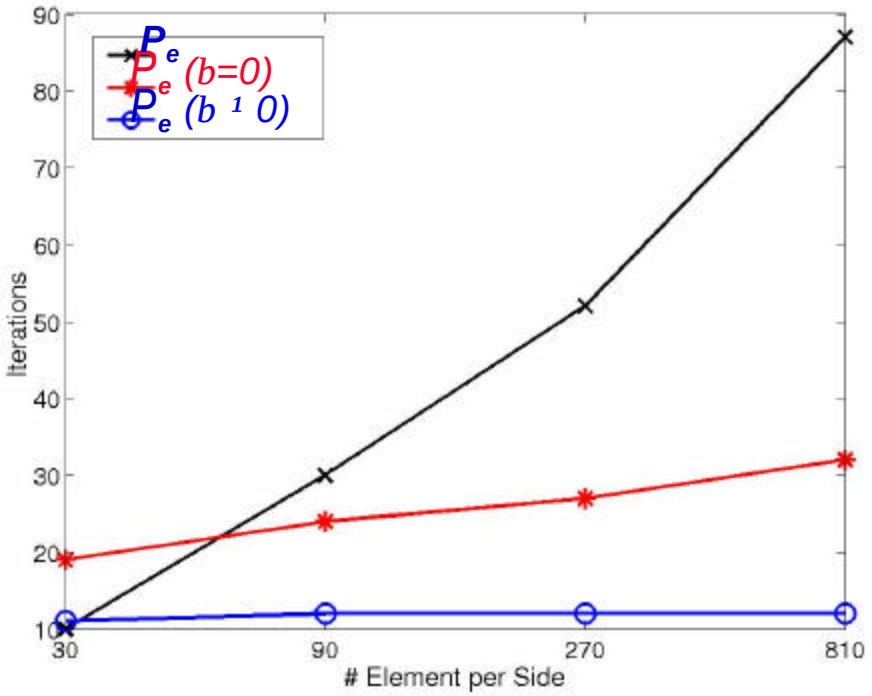

3D Cube, $\sigma = 10^{-3}$

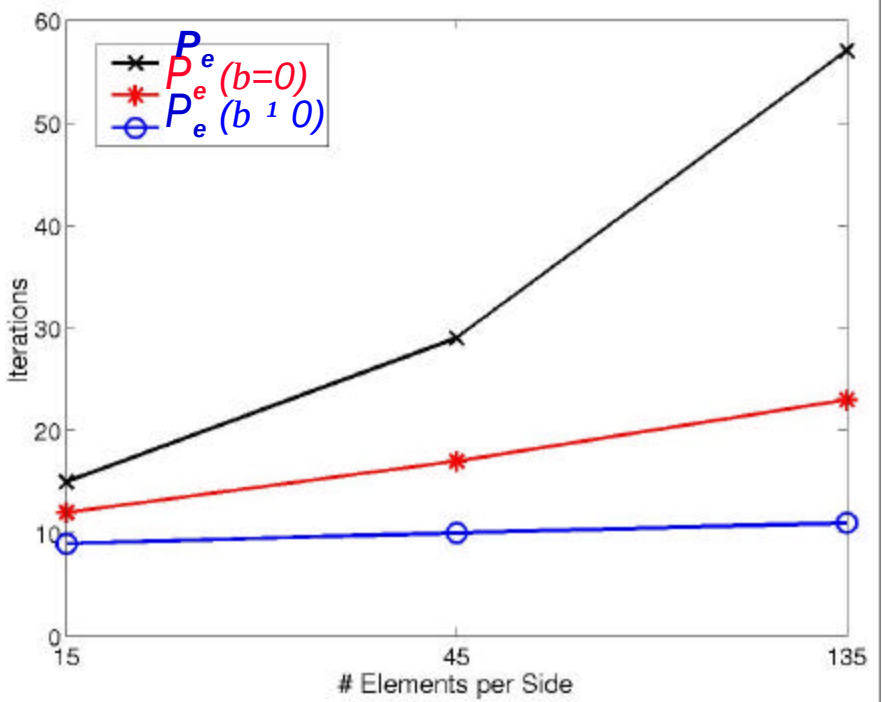

CG, W(1,1) cycle, $\|r\|_T / \|r_0\|_T \leq 10^{-8}$

complexity $\leq$ { 1.15 in 2D ; 1.11 in 3D

3D Circuit Equation Coupling Algorithm

- **External circuit and mesh need to be able to be coupled.**
- **Coupling in 3D ALEGRA-MHD is based on generating an equivalent circuit element using the weak form of the diffusion equation in the form of an energy equation.**
- **Current is linear in the boundary conditions. Generate two solutions leading to a parameterized solution as a function of the current at the end of the time step.**
- **Fit to a lumped circuit element by choosing an L and an R to match the instantaneous inductance and the energy transfer to/from the mesh.**
- **Solve the external lumped element circuit equation to obtain a new I.**
- **The new field is then a linear combination of the two solutions.**

Mesh element representation.

- **Match the volume integrals associated with the discrete Poynting flux with a circuit representation.**

$$\Delta t\,(b_1 \hat{I} + b_2 \hat{I}^{\,2}) = \int_0^{\Delta t} (L\dot{I} + R I)\, I\, dt$$

$$\hat{I} = I_0 + \dot{I}\Delta t = I_0 + d\,I$$

$$I = I_0 + \dot{I}t$$

- **Evaluate in orders of** $\mathrm{d}\mathbf{I}$

$$b_1 + b_2 I_0 = R I_0$$

$$\Delta t b_2 = L$$

- **Energy error will appear at O((**d**I)^2**). However, choose the resistance so that discrete energy is conserved for a linear current.**

The remap step

- **The Lagrangian step maintains the discrete divergence free property via flux updates given only in term of curls of edge centered circulations.**
- **The remap should not destroy this property of the magnetic field representation.**
- **Constrained transport (CT) developed by Evans and Hawley is the prototype algorithm for advection consistent with the divergence free constraint.**

CT on unstructured quad and hex grids (CCT)

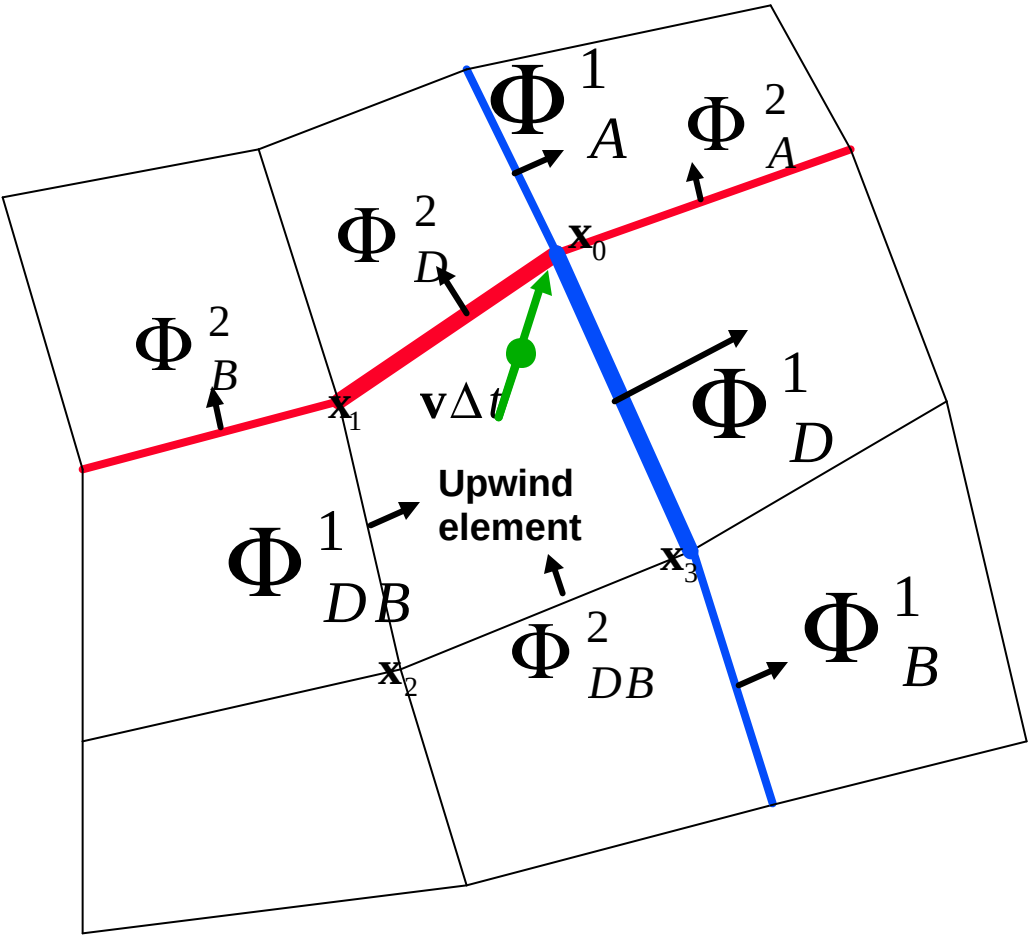

- **Electric field updates are evaluated by computing an approximation to the flux through the upwind characteristic (green dot quadrature point).**
- **Take curl to get updated fluxes.**
- **Requires tracking flux and circulation sign conventions.**
- **High order methods use more information that just the donor fluxes shown.**

- **Evans and Hawley CT uses flux information on blue and red faces on a Cartesian grid.**

Face element representation

- **Need representation of upwind element in terms of the reference coordinates of a linear element.**

$$\mathbf{x} = (\mathbf{x}_0 + x(\mathbf{x}_1 - \mathbf{x}_0)) + h[(\mathbf{x}_3 + x(\mathbf{x}_2 - \mathbf{x}_3)) - (\mathbf{x}_0 + x(\mathbf{x}_1 - \mathbf{x}_0))]$$

$$\mathbf{B} = \sum_f \Phi_f \mathbf{F}_f = \frac{\Phi^1_D (x-1)\frac{\partial \mathbf{x}}{\partial x}}{\frac{\partial \mathbf{x}}{\partial x} \times \frac{\partial \mathbf{x}}{\partial h}} + \frac{-\Phi^1_{DB} x \frac{\partial \mathbf{x}}{\partial x}}{\frac{\partial \mathbf{x}}{\partial x} \times \frac{\partial \mathbf{x}}{\partial h}} + \frac{\Phi^2_D (h-1)\frac{\partial \mathbf{x}}{\partial h}}{\frac{\partial \mathbf{x}}{\partial x} \times \frac{\partial \mathbf{x}}{\partial h}} + \frac{-\Phi^2_{DB} h \frac{\partial \mathbf{x}}{\partial h}}{\frac{\partial \mathbf{x}}{\partial x} \times \frac{\partial \mathbf{x}}{\partial h}}$$

- **Integrate over flux surface.**

$$\int_{S_i} d\mathbf{x} \times \mathbf{B} \approx dh(\Phi^1_D + \tfrac{dx}{2}(\Phi^1_{DB} - \Phi^1_D)) - dx(\Phi^2_D + \tfrac{dh}{2}(\Phi^2_{DB} - \Phi^2_D))$$

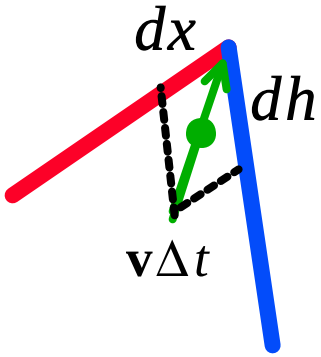

- **Face normal gradient terms appear. These do not appear with EH CT.**

Characteristic constrained transport (CCT)

- **We now have a representation for the edge magnetic flux contribution.**
- **Compute** dx, dh **to first order**

$$-\mathbf{v}\Delta t = dx\,(\mathbf{x}_1 - \mathbf{x}_0) + dh\,(\mathbf{x}_3 - \mathbf{x}_0)$$

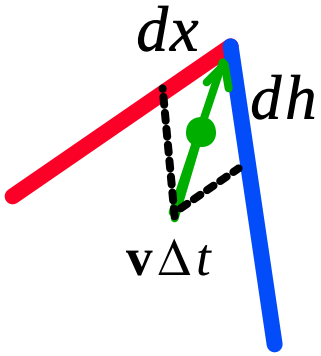

- **There is no natural variation tangential to the face. Need high order reconstruction in this direction.**

$$\hat{\Phi}^1(h) = \Phi^1_D + (A^1_D)^2\, s^1(\tfrac{1}{2} - h) \qquad \hat{\Phi}^2(x) = \Phi^2_D + (A^2_D)^2\, s^2(\tfrac{1}{2} - x)$$

- **For unstructured grids a type of cross face tangential gradient limiting analogous to ALEGRA geometry independent volumetric limiting was implemented.**
- **This cross face reconstruction mimics the EH ideas for Cartesian grids**
- **Several limiters have been implemented (Van Leer, harmonic, minmod, donor)**

CT 1D advection

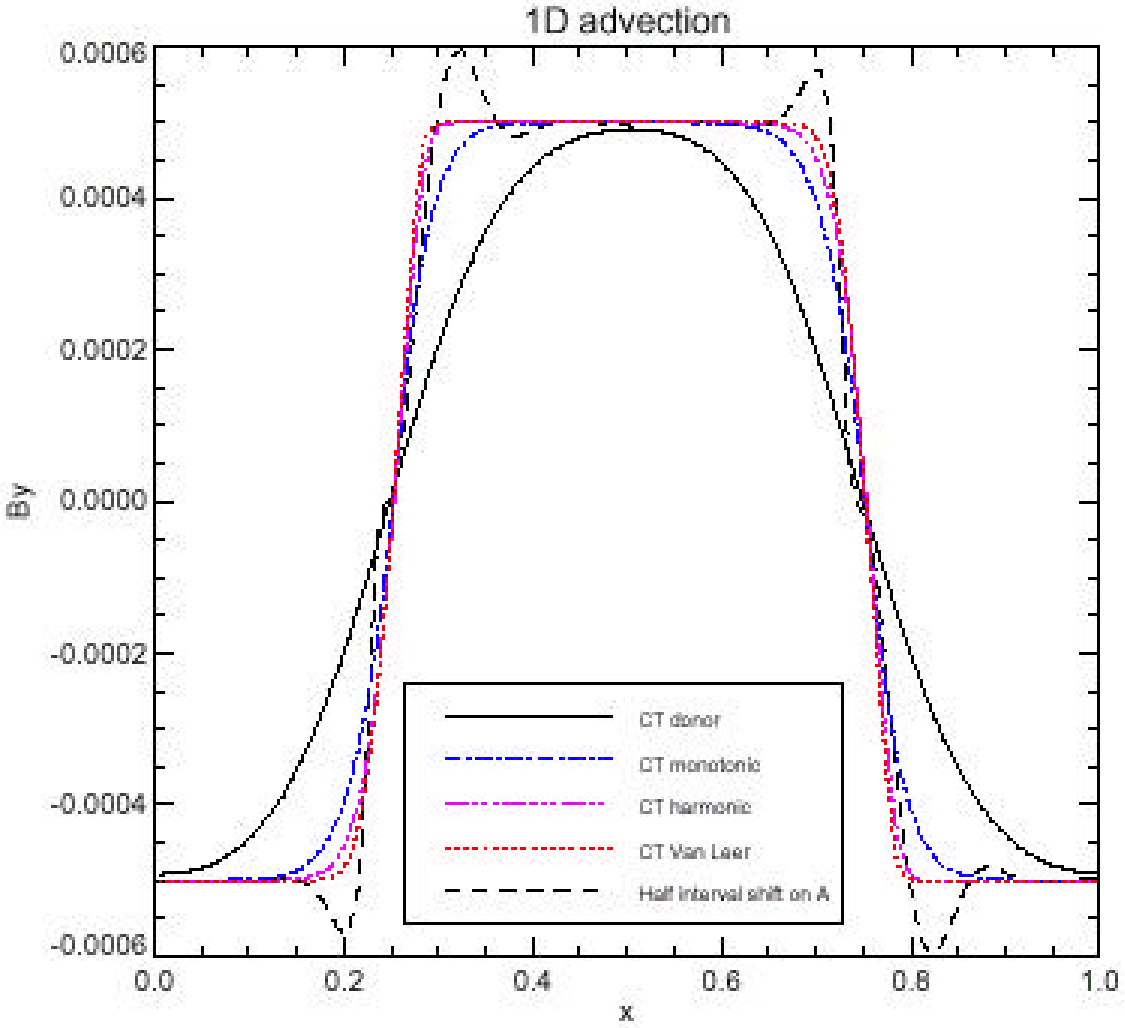

EH-CT

- **25x25 cartesian mesh - harmonic limiting**

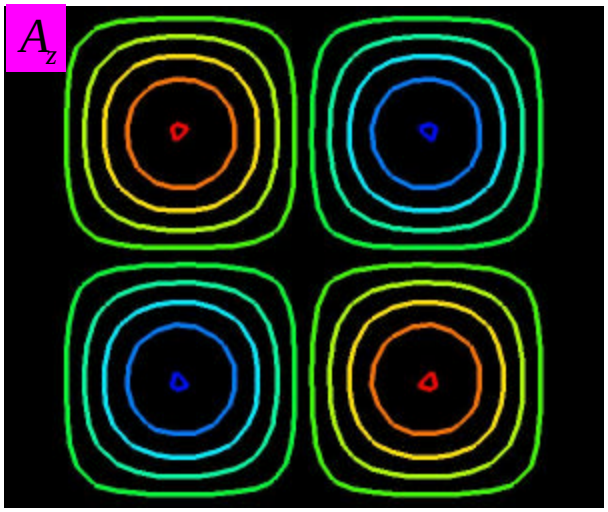

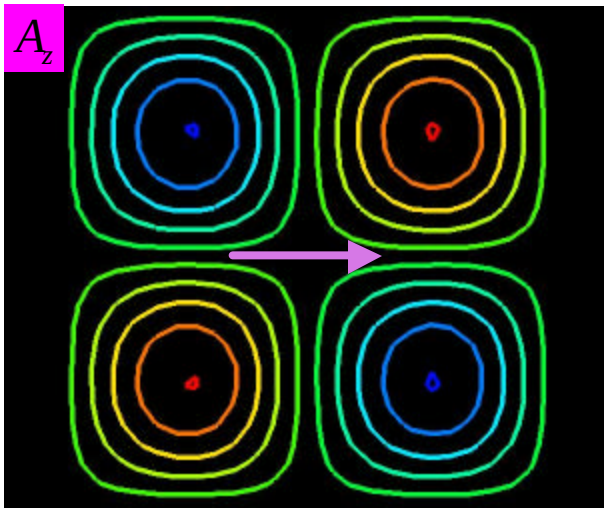

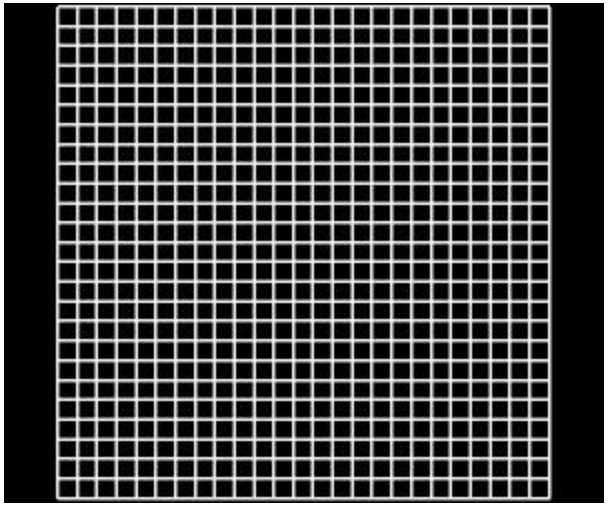

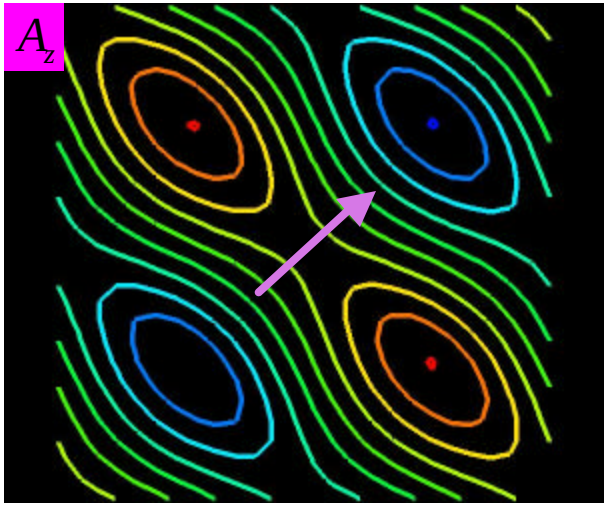

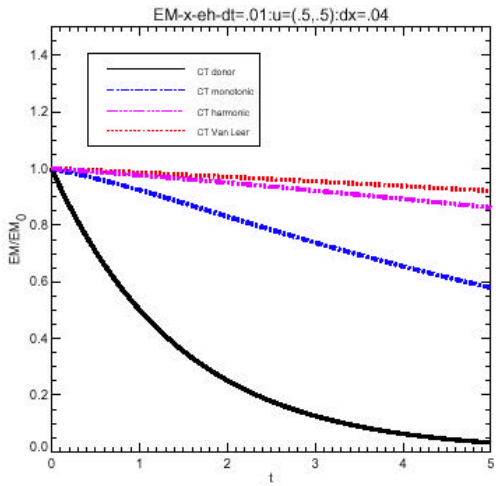

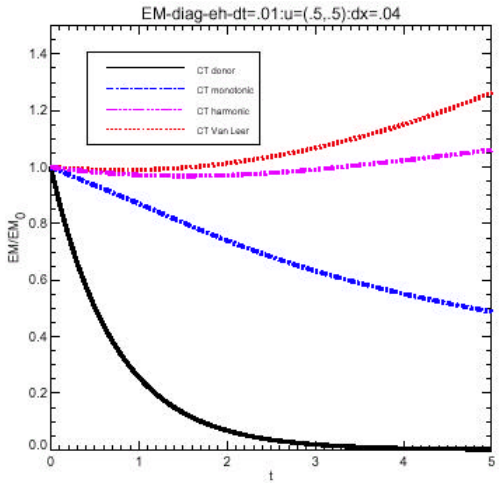

CCT on Cartesian grid

- **EXCELLENT RESULTS- diagonal, slant or grid aligned**

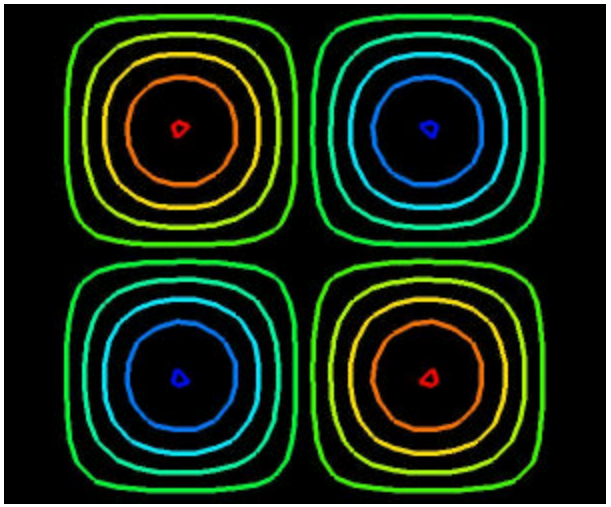

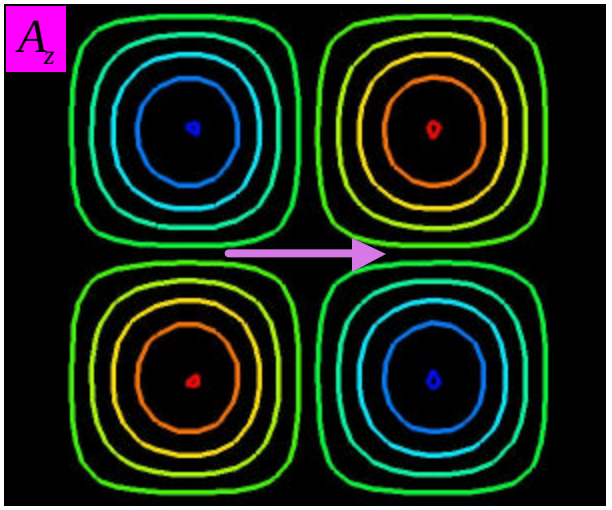

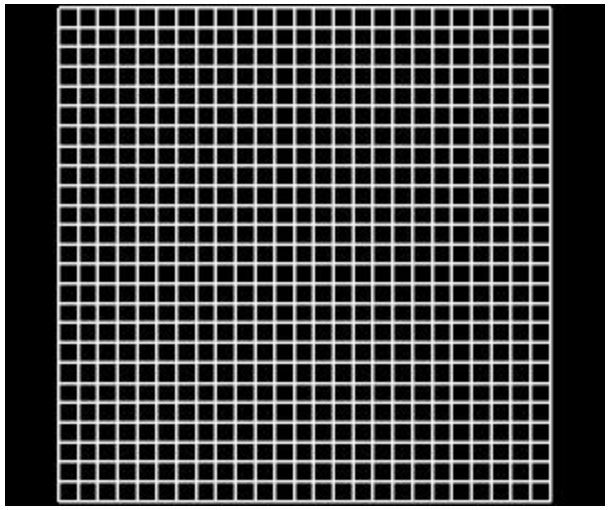

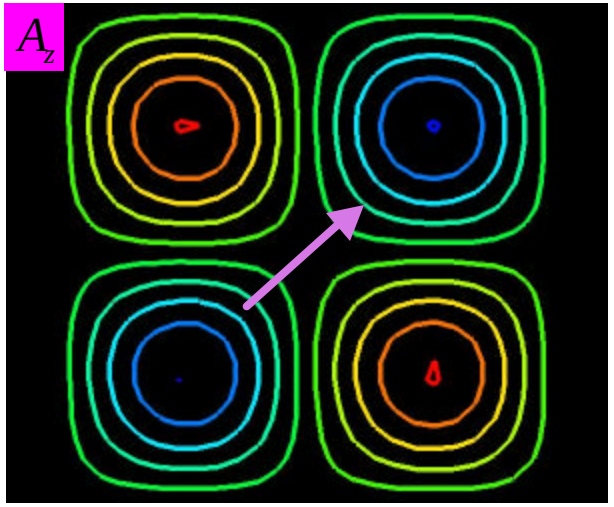

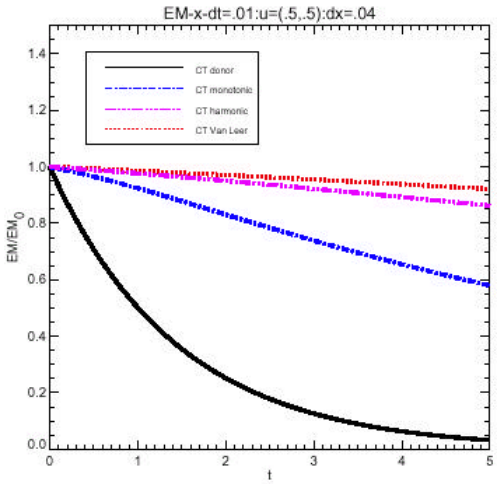

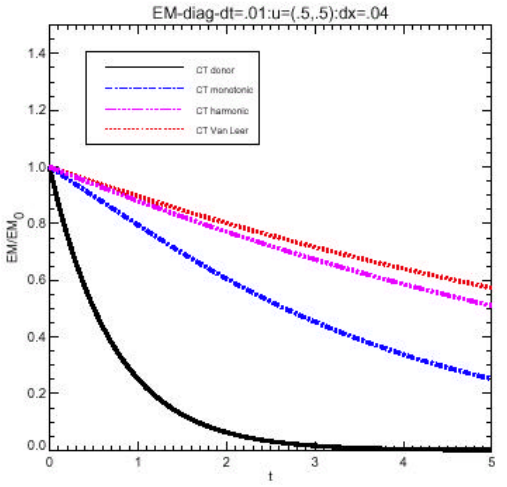

CCT on distorted or unstructured grids

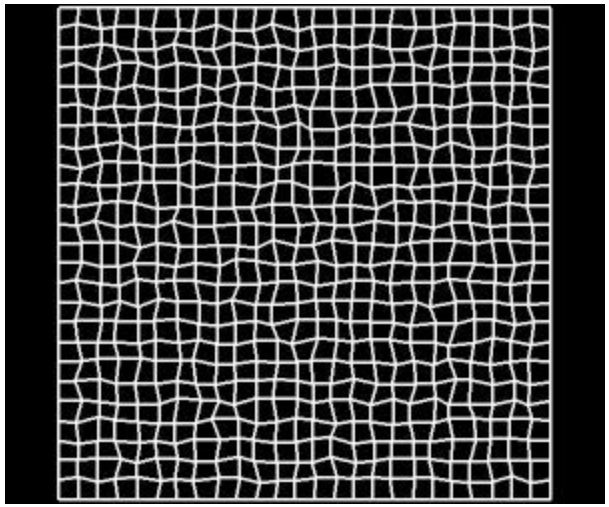

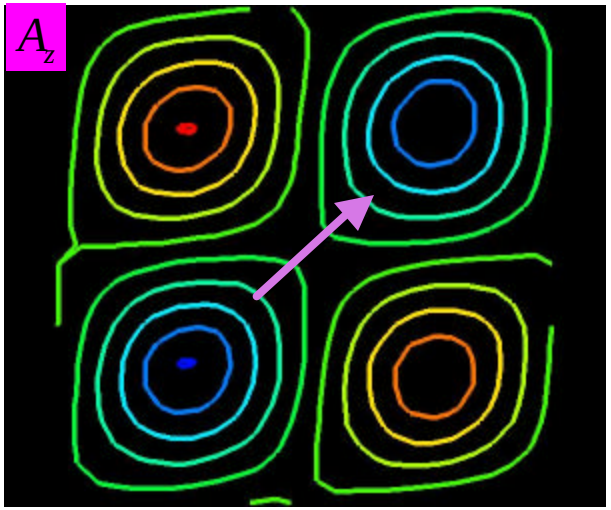

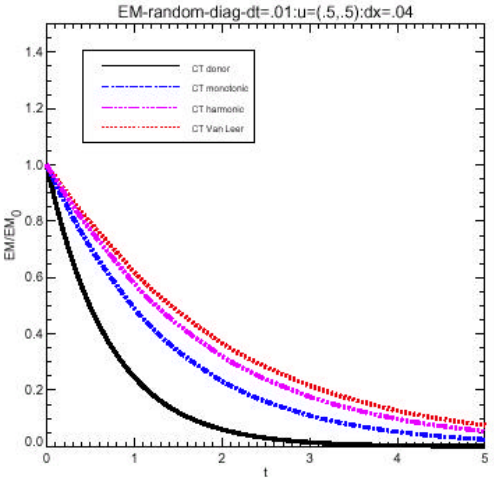

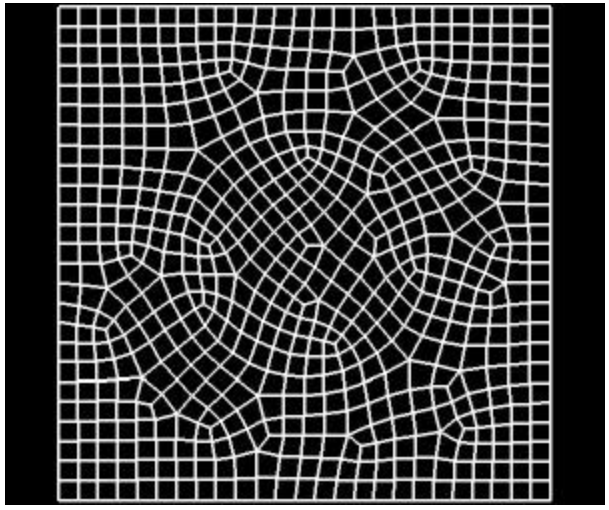

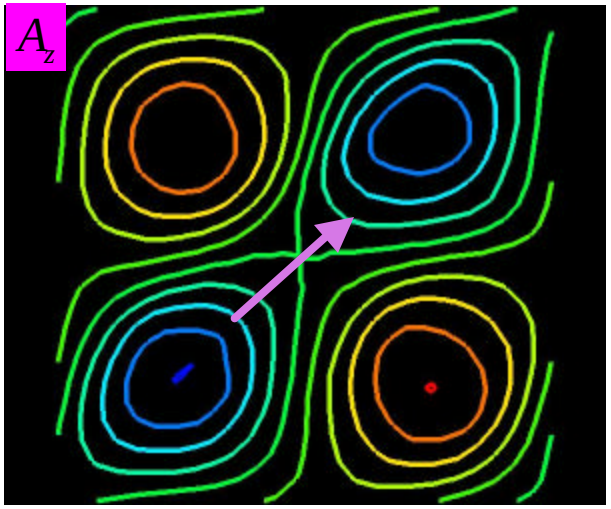

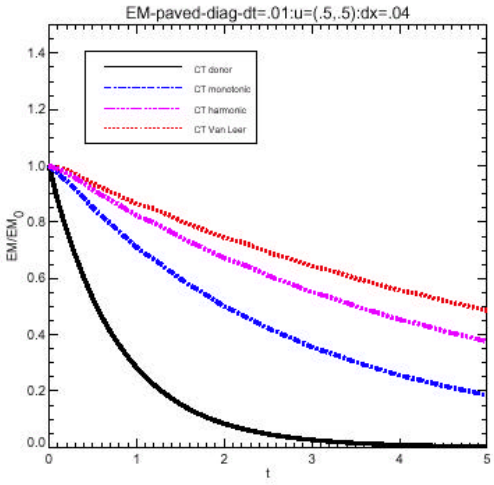

- **ACCURATE limited gradients in the cross face direction are required in the general grid case.**

Improved CCT Algorithm

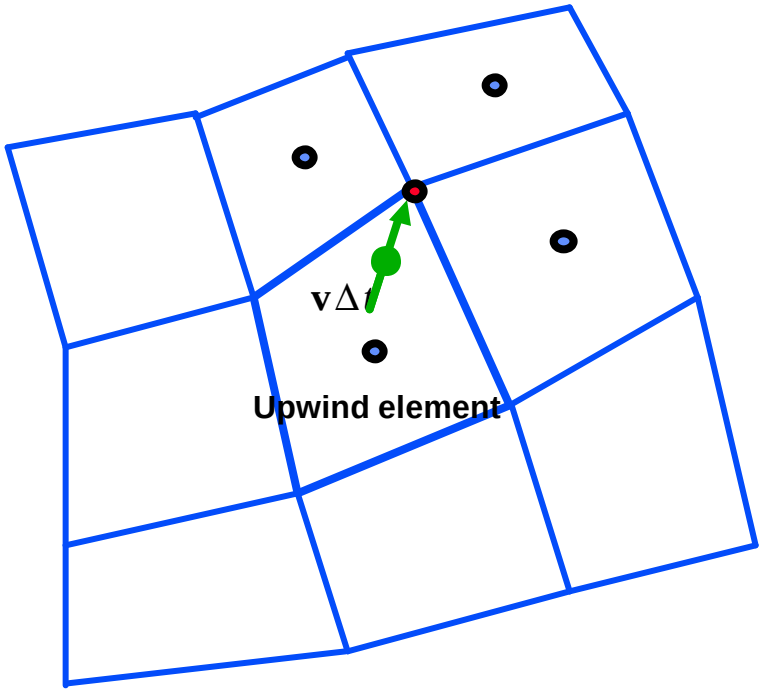

- **Compute B at nodes from the face element representation at element centers. This must be second order accurate. Patch recovery (PR) suggested.**
- **Compute trial cross face element flux coefficients on each face using these nodal B.**
- **Limit on each face to obtain cross face flux coefficients which contribute zero total flux.**
- **Compute the edge flux contributions in the upwind element by a midpoint integration rule at the center of the edge centered motion vector. (green line).**
- **Note: The current face based 3D algorithm does not take into account variations of the fluxes in the upwind edge direction but is naturally included here.**
- **Work is in progress.**

- **CRITICAL QUESTION: What is the best procedure to compute an accurate B at the nodes from an arbitrary patch of low order face elements? Is it provably accurate?**

Patch Recovery Based CCT

CT donor
CT Van Leer
PR CT harmonic
CT monotonic
CT harmonic

Cartesian | **Paved** | **Randomized**

diag

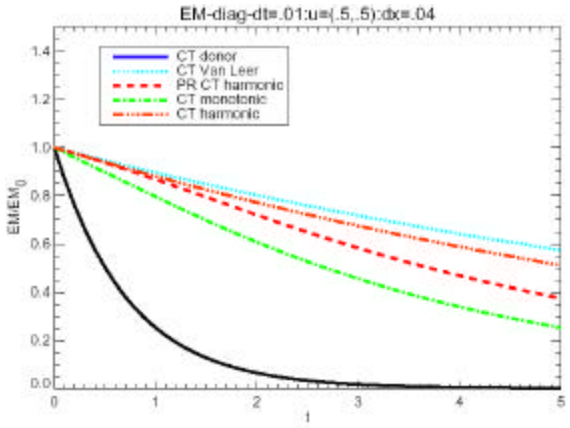

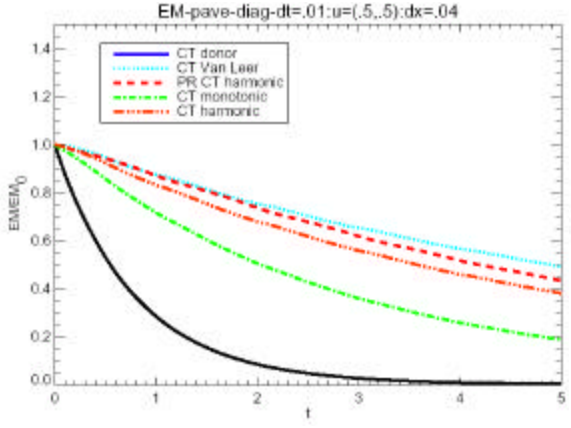

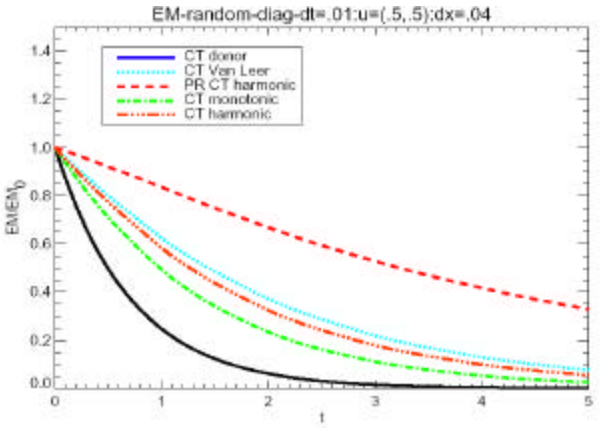

x

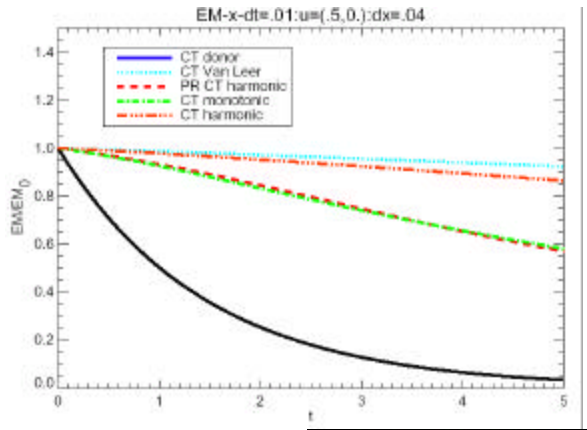

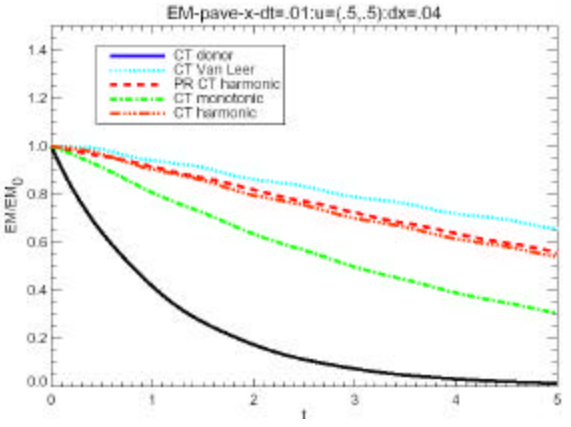

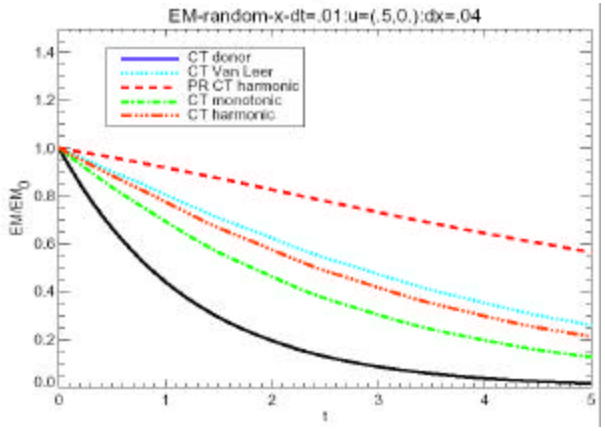

Paved,diagonal, face based, harmonic

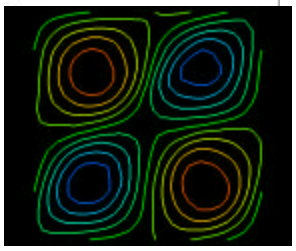

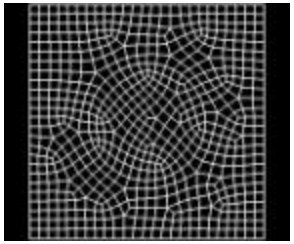

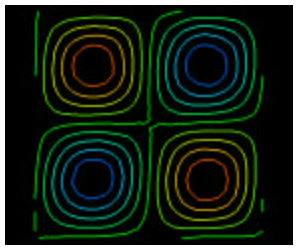

Paved,diagonal, patch recovery, harmonic

Algorithmic Summary

- **Vector finite elements for representing the magnetics is a natural match for developing a resistive MHD ALE algorithm.**
- **AMG methodologies are being implemented with considerable success for the diffusion solve.**
- **Constrained transport algorithms can be built in a natural way based on face element representations.**
- **The approach described provides a robust foundation for meeting the challenges of 3D Z-pinch MHD modeling.**
- **Future activities/needs: improved CCT, tensor thermal and magnetic transport coefficients, better time step controls, h-adaptivity**

Physical Insight Into Observed Phenomenon

• Axially-varying streams of pre-cursor material from wires observed at early time.

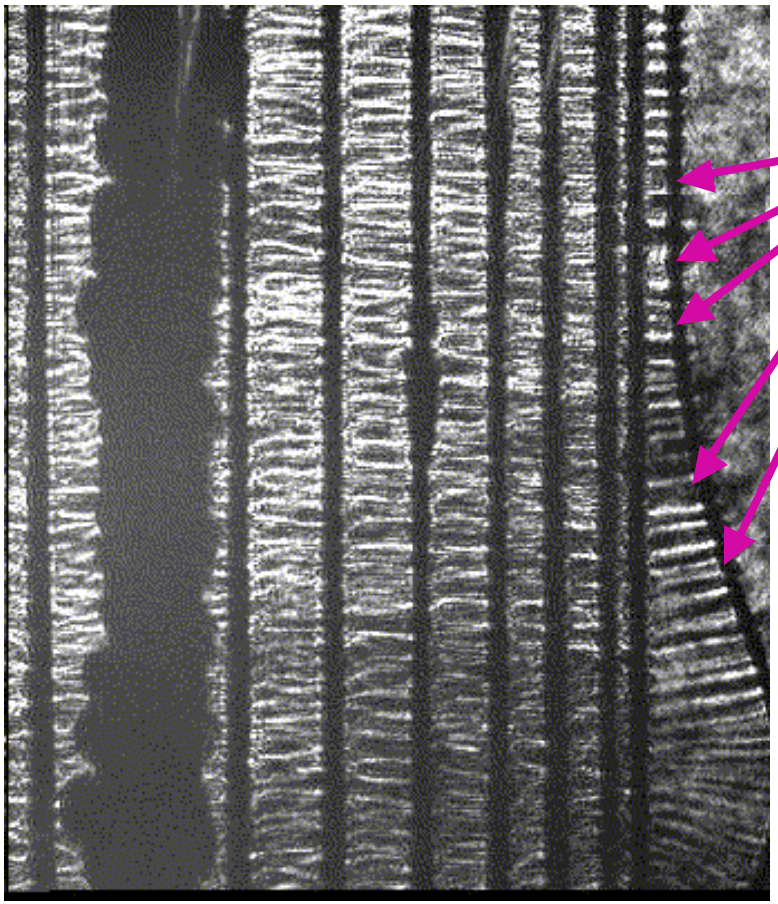

Image supplied by Sergey Lebedev, Imperial College

Details:

- Finite spacing between the streams of ablated mass.
- Flow is nearly orthogonal to wire.

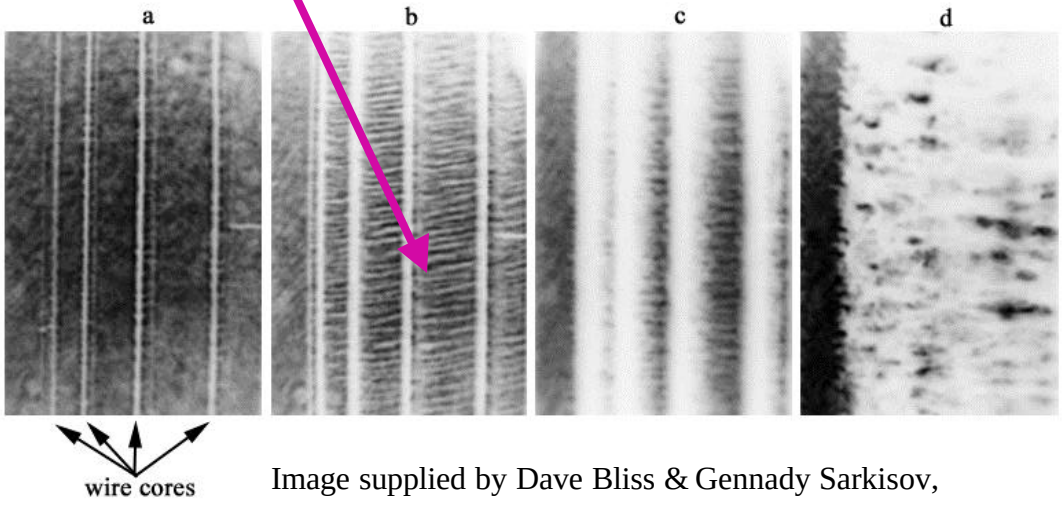

Image supplied by Dave Bliss & Gennady Sarkisov, Sandia National Laboratories

Sinusoidal Core Perturbation

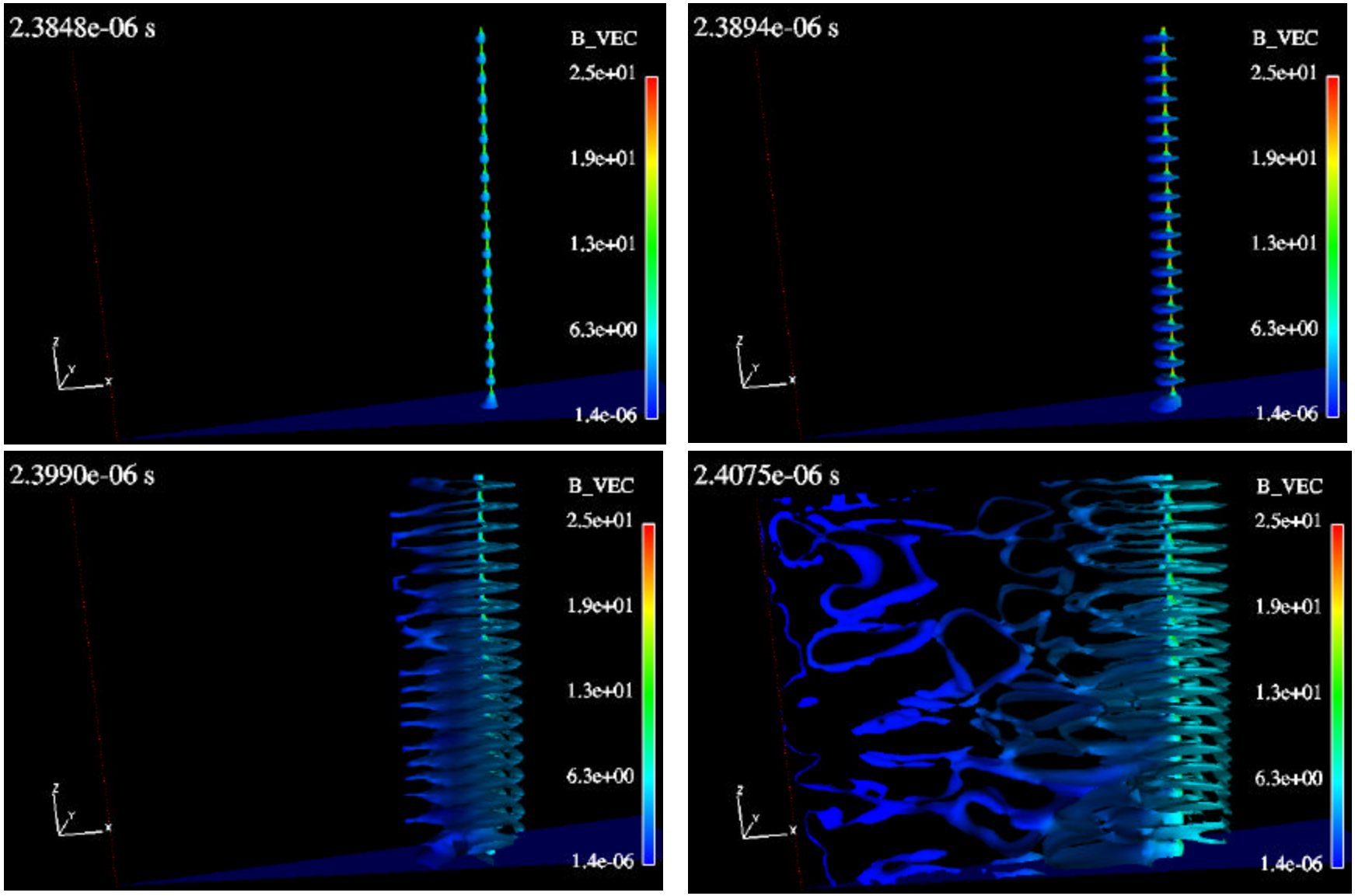

Volume fraction isosurface (elements 70% filled) with magnetic field strength coloring

Valuable Physical Insight

Wire ablation dynamics governed by interplay between global & local magnetic fields.

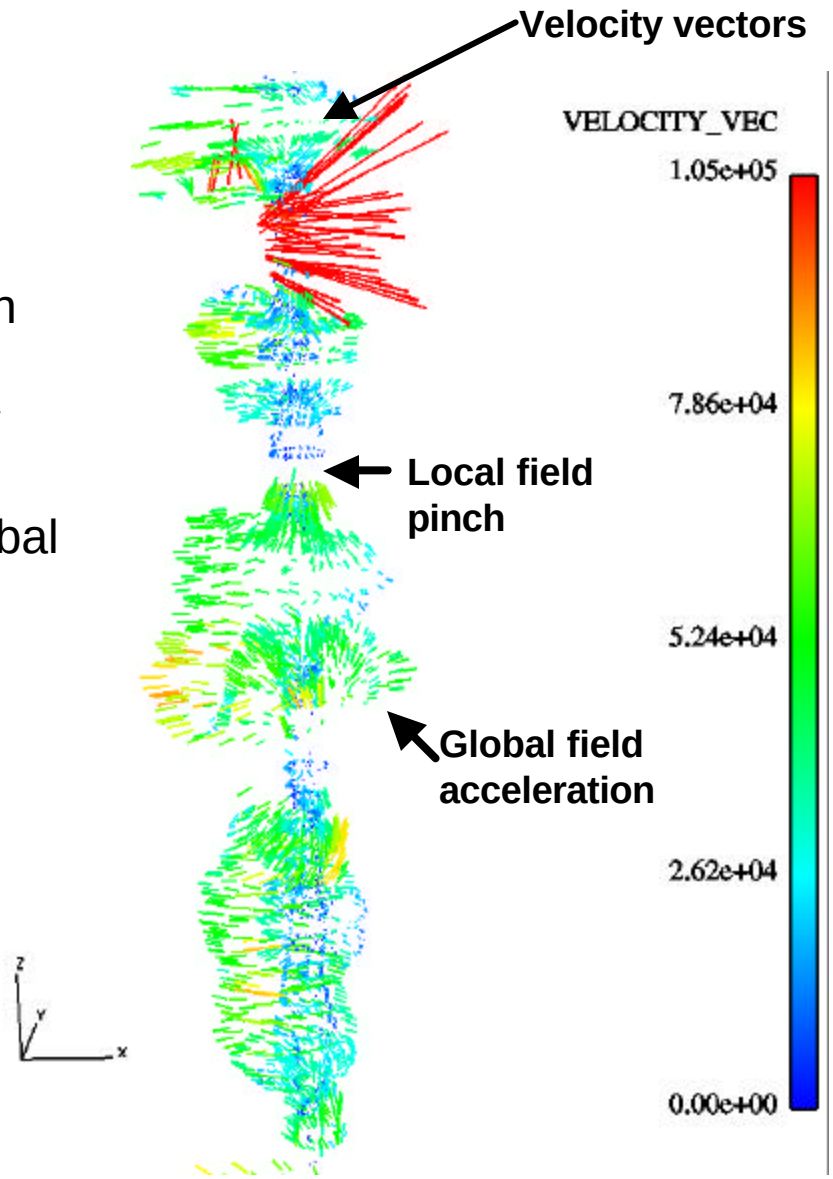

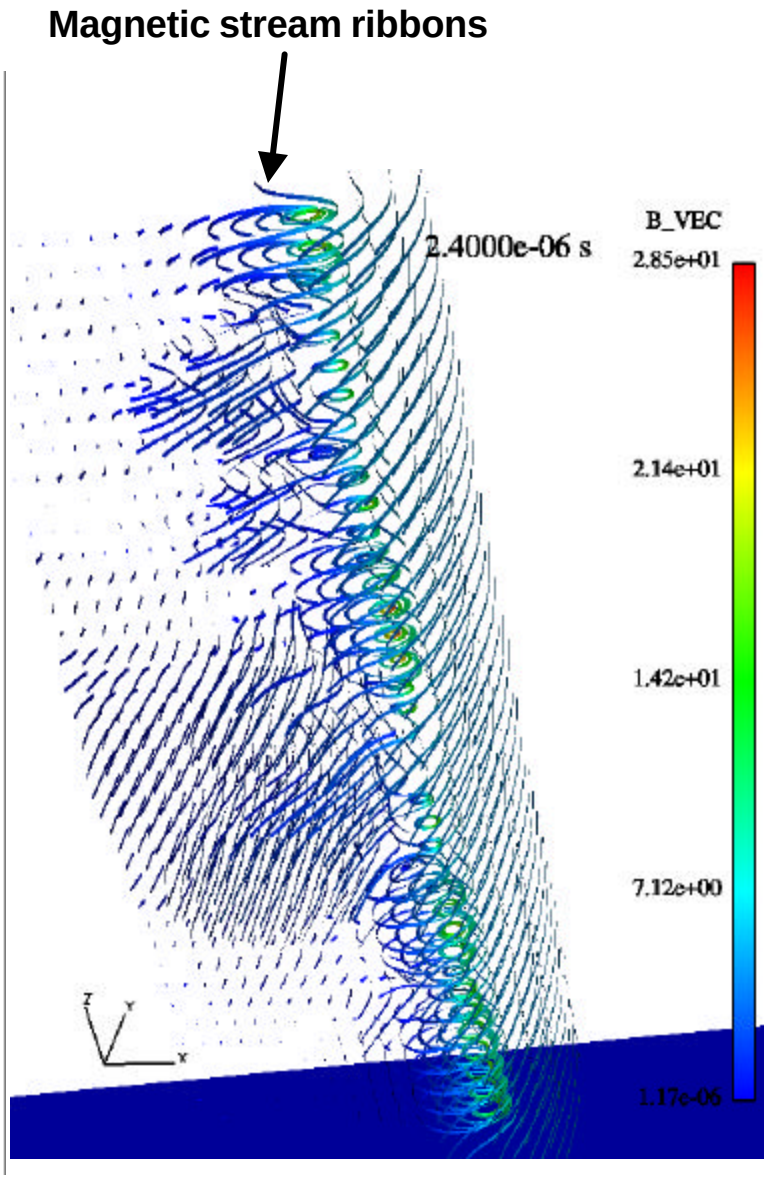

Observed/Simulated Phenomenon

• Axially-varying streams of pre-cursor material from wires observed at early time.

Details:

- Finite spacing between the streams of ablated mass.
- Flow is orthogonal to wire.

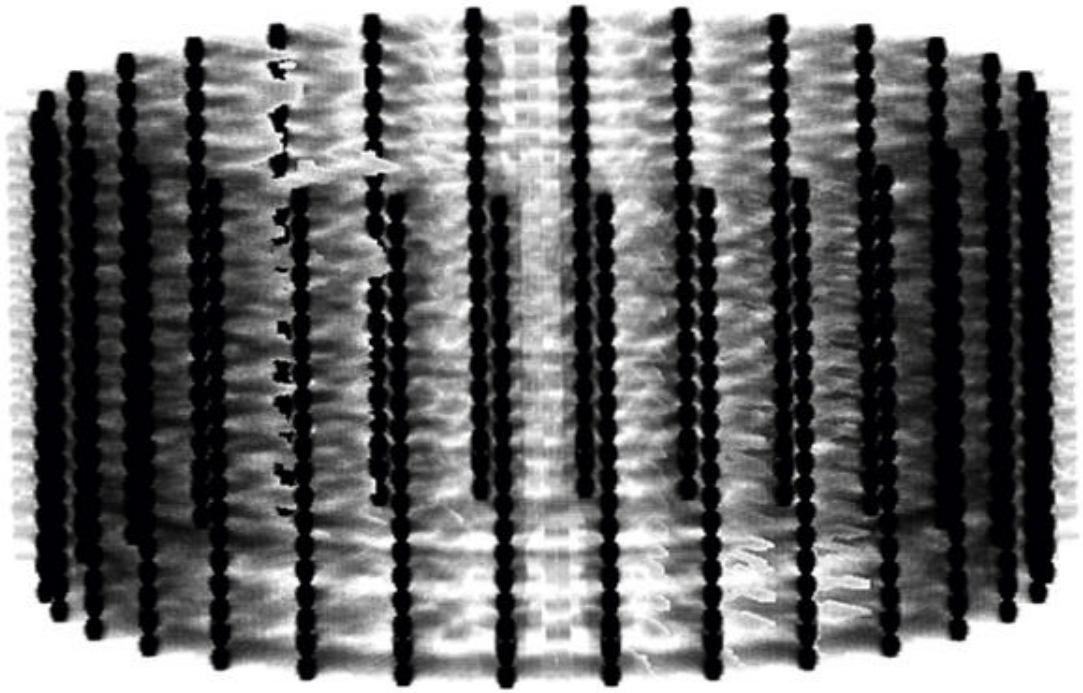

Volume rendering of 30-wire sinusoidal perturbation simulation (density used as “opacity”); image generated using TNTvol

Image supplied by Sergey Lebedev, Imperial College

Application Summary

- **Significant MHD algorithmic advances provide unique 3D HEDP simulation capability for Z-pinch environments.**
- **Present: Gaining new insight into Z-pinch dynamics & understanding of wire ablation and pinch physics.**
- **Goal: Utilize simulations to guide experimental program & assist with new machine acquisition.**

References

•**Bochev, Robinson, Hu, Tuminaro, "Toward Robust 3D Z-pinch simulations: Discretization and Fast Solvers for Magnetic Diffusion in Heterogeneous Conductors," Electronic Transactions Numerical Analysis, 15 (2003), pp. 186-210.**

•**P. B. Bochev, C. J. Garasi, J. J. Hu, A. C. Robinson and R. S. Tuminaro, " An Improved Algebraic Multigrid Method for Solving Maxwell's Equations," accepted SIAM J. Scientific Computing.**

•**R. W. Lemke, M. D. Knudsen, A. C. Robinson, T. A. Haill, K. W. Struve, J. R. Asay, and T. A. Mehlhorn, "Self-consistent, two-dimensional, magneto-hydrodynamic simulations of magnetically driven flyer plates," Physics of Plasmas, Volume 10, Number 5, May 2003.**

•**P. B. Bochev and A. C. Robinson, "Matching Algorithms with physics: exact sequences of finite element spaces," Collected Lectures on the Preservation of Stability under Discretization, D. Estep and S. Tavener, Eds., SIAM, Philadelphia, 2002.**

•**Robinson, Bochev, Rambo, "Constrained Transport Remap on Quadrilateral and Hexahedral Grids," Presentation at SIAM National Meeting, San Diego, July 2001.**

•**Peery and Carroll, "Multi-Material ALE methods in unstructured grids," CMAME,187, 2000, pp. 591-619.**

•**C. R. Evans and J. F. Hawley, "Simulation of magnetohydrodynamic flows: a constrained transport method," The Astrophysical Journal, 332, Sept. 1988, pp 659-677.**

Acknowledgements

- **Analysts – Chris Garasi, Ray Lemke**
- **Vector FE/CT – Pavel Bochev**
- **H(curl) multigrid - Jonathan Hu, Ray Tuminaro**
- **2D vector potential remap (CT) -Peter Rambo LLNL**
- **MHD code development – Tom Haill**
- **Sandia HEDP working group.**
- **Nevada (ALEGRA) framework team contributers.**

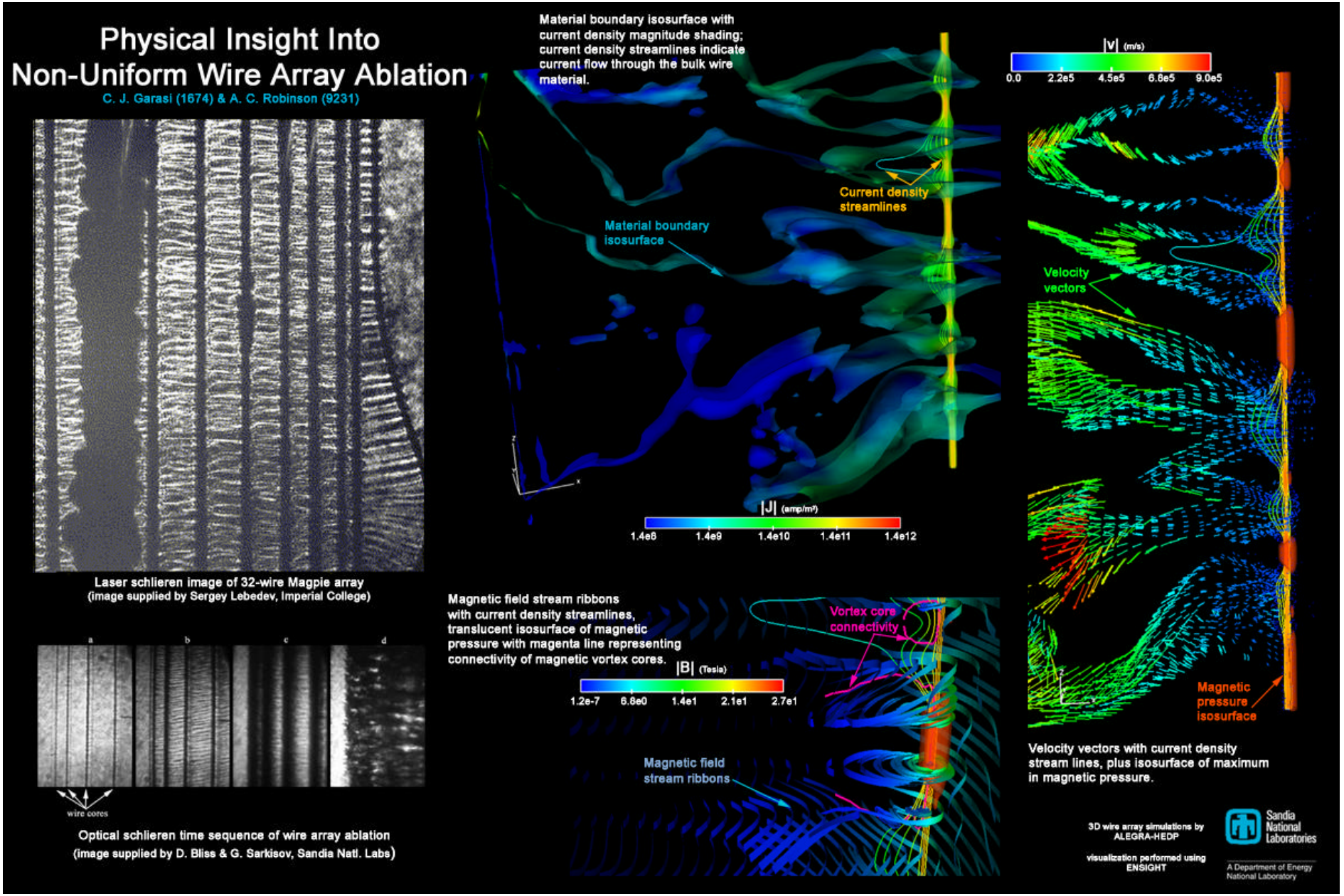

Still Image for Poster and Buneman Competition

Buneman Animation Contribution

These slides contain representative information from the MPEG movie generated

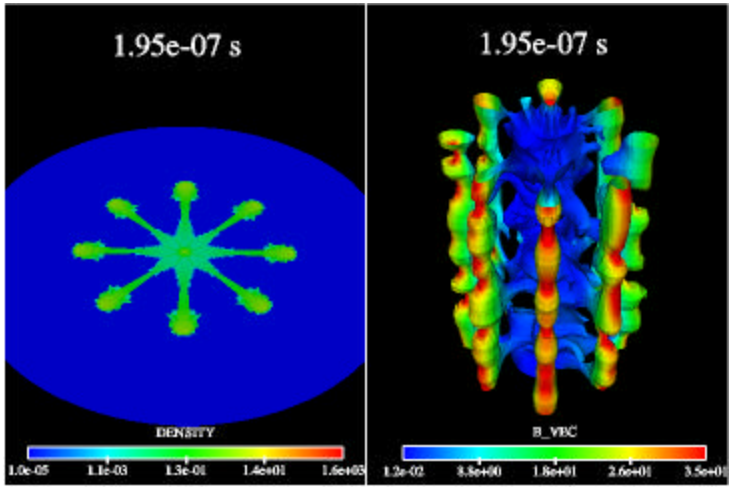

8-wire 3D calculation with time sequence and image rotations

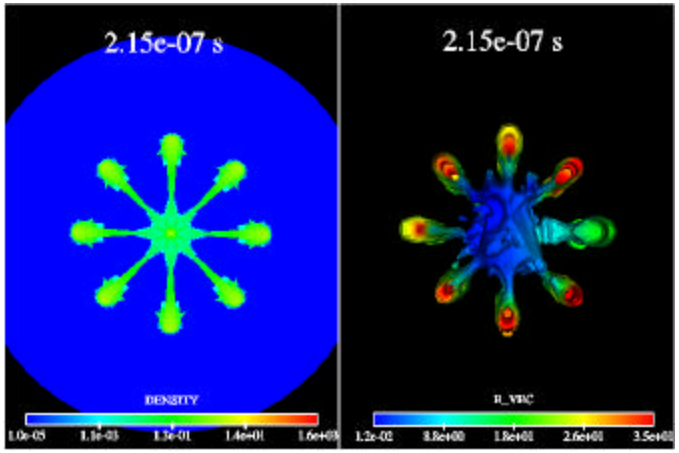

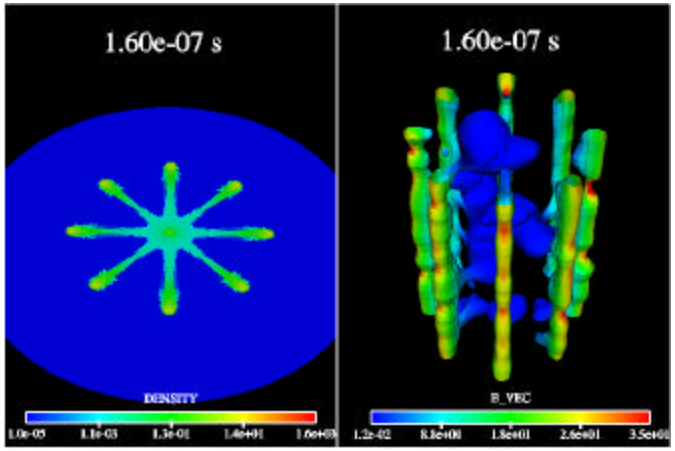

Buneman Animation Contribution (2)

These slides contain representative information from the MPEG movie generated

Image rotations

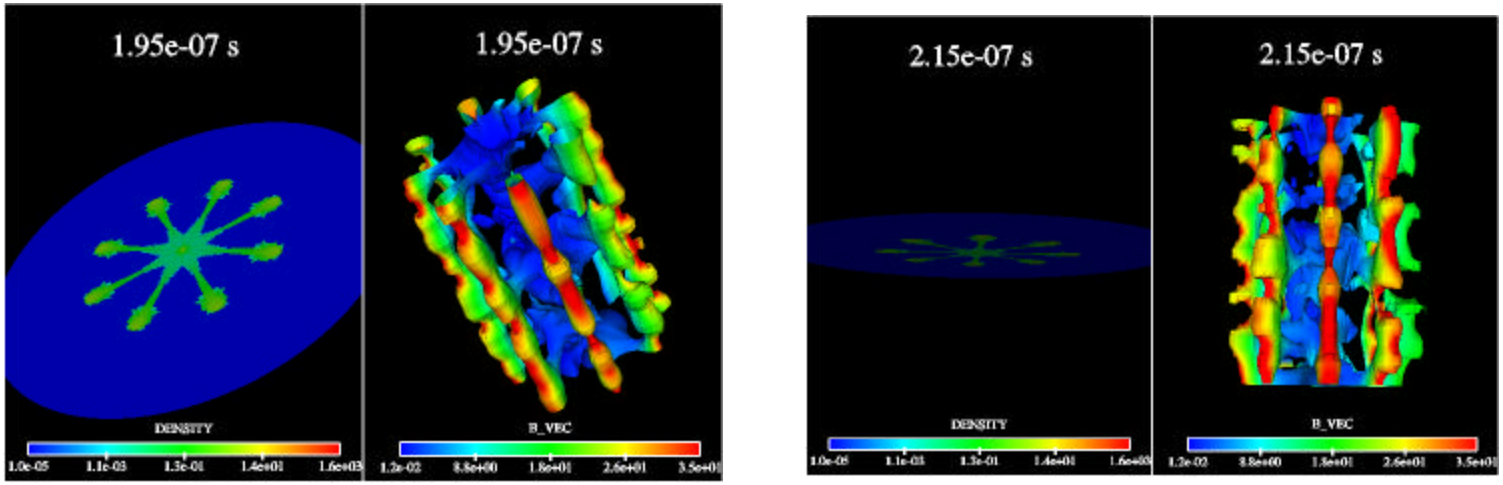

Buneman Still Image Competition Submission
"Physical Insight Into Non-Uniform Wire Array Ablation"
Christopher Garasi & Allen Robinson
Sandia National Laboratories[a]

The Figure contains multiple visualizations to assist in the understanding of non-uniform wire array ablation seen in experimental images. The two left-most images are schlieren images of wire arrays on the MAGPIE accelerator (Imperial College) and the Z machine (Sandia National Labs). These images clearly display low density ablation of wire material traveling to the center of the wire array. This material ablates non-uniformly along the length of each wire with a nearly uniform wavelength of perturbation. The visualizations in the Figure help to understand the physics which maintains this type of ablation.

The upper central image shows results from a 3D ALEGRA-HEDP (high energy density physics) simulation of a wire in a 30-wire periodic array. The material boundaries are represented as a translucent isosurface color shaded with the magnitude of the current density (J). Current density streamlines also are illustrated in order to visualize the direction of the current flowing through the wires. Although the majority of the current is flowing through the wire core, some current is advected with the low density material ablated from the wire.

The right-most image also displays current density streamlines as well as a translucent isosurface of the maximum magnetic pressure. Velocity vectors (V) have been added in order to show the magnitude and direction of the ablated material flow. Regions of increased magnetic pressure squeeze the wire material due to enhanced local magnetic field. This causes material to travel along the wire until it reaches an area where the global magnetic field of the array dominates. The global field causes the ablated material to travel radially inward due to magnetic forces. The simulation was initialized with a random wire surface perturbation which causes areas with increased local magnetic field versus global field to develop.

The final image in the lower center focuses on a portion of the wire and illustrates the magnetic field (B) topology using magnetic field stream ribbons. Current density streamlines provide continuity between all the visualizations as a point of reference. An additional technique involving the visualization of vortex cores derived from the magnetic field was used to illustrate the interaction between the flow and the magnetic field topology. Vortex cores for the initial magnetic field distribution would connect the nulls of the field through the center of the wire. As the non-uniform flow establishes itself, the magnetic field is advected toward axis non-uniformly, causing increased magnetic tension. The line representing the connectivity of the vortex cores illustrates how the field uniformity in the z-direction has been altered due to advection at various distance along the wire. The vortex core line, which was initially straight and continuous, has broken as a result of the advection of the field due to mass ablation while the regions with increased local field have remained about the wire.

In conclusion, this Figure uses visualization of scientific quantities in order to help our understanding of the mechanism which maintains the wire ablation pattern seen in experimental images. Although the source of the initial perturbation is not well understood at this point in time (and might not even be an MHD effect), it is the variation in the strength of the local and global magnetic field about each wire in the array which establishes this steady flow of ablated material. The ablated material does carry a small fraction of the current toward the array center, however the majority of the current still runs in the wires. Additionally, the current carrying material also advects magnetic field toward the center of the array causing increased magnetic tension with those regions about the wire where the topology has not changed. Eventually, the array loses enough mass and magnetic forces are strong enough to cause the array to collapse onto this pre-fill material.

[a] Sandia is a multiprogram laboratory operated by Sandia Corporation, a Lockheed Martin Company, for the United States Department of Energy's National Nuclear Security Administration under contract DE-AC04-94AL85000.